Energetically competitive growth patterns of silicon clusters: Quasi-one-dimensional clusters versus diamond-like clusters

P. L. Tereshchuk,* Z. M. Khakimov,† and F. T. Umarova
Institute of Nuclear Physics, Uzbekistan Academy of Sciences, Tashkent 702132, Uzbekistan

M. T. Swihart
Department of Chemical and Biological Engineering, University at Buffalo (SUNY), Buffalo, New York 14260-4200, USA
(Received 15 December 2006; revised manuscript received 25 April 2007; published 17 September 2007)

Silicon clusters with a diamond-like core and energetically competitive non-diamond clusters were studied using the nonconventional tight-binding molecular dynamics simulation method. Non-diamond clusters were constructed according to a quasi-one-dimensional pentagon-based regular growth pattern. A nontrivial competition between surface and core reconstructions in the clusters, in order to reach energetically favorable atomic arrangements, was observed. This prevents unlimited growth via the one-dimensional pattern. Starting from Si_{43}, there was substantial deviation from the stacked pentagon motif, and for Si_{61}, one end of these clusters became almost two-dimensional. Clusters with a diamond-like core were subjected to substantial reconstruction. These were energetically unfavorable relative to non-diamond clusters for the sizes considered ($\leqslant$71 atoms). The importance of capped pentagon motifs in the surface reconstruction for energetically competitive nanometer-size diamond-like clusters was demonstrated. A lower bound of 115 atoms for the transition from non-diamond structure to diamond-like structure is estimated by extrapolation of the present results.

DOI: 10.1103/PhysRevB.76.125418 PACS number(s): 71.15.Nc, 61.46.−w, 73.22.−f

I. INTRODUCTION

Nanometer-size silicon clusters have attracted much attention, ever since the observation of efficient luminescence from porous silicon,[1] due to their potential use as light emitters in displays or general illumination and as fluorescent probes for bioimaging. To date, Si nanoparticles ranging from 1 to 5 nm in diameter have been prepared by a variety of methods[2–7] and were found to exhibit photoluminescence at wavelengths ranging from blue to the near infrared. The core of luminescent Si nanoparticles is commonly presumed to be diamond-like as in bulk silicon, with each silicon atom surrounded symmetrically by four other Si atoms that form a perfect tetrahedron. The smallest (1 nm in diameter) model of luminescent Si particles is a H-terminated, reconstructed Si_{24} cage with one silicon tetrahedron in the interior,[8] that is, $Si_5Si_{24}H_{24}$. The perfect diamond-like coordination of Si atoms, at least up to this size, can be stabilized only by termination of surface dangling bonds by hydrogen or other atomic or molecular species. Bare clusters, containing up to seven Si atoms, are compact clusters,[9] while larger clusters tend to have prolate shapes.[10] The particles are again spherical for numbers of atoms in the range[10] from 20 to 30, but they have little resemblance to the bulk silicon structure. Moreover, globally minimum energy clusters that differ in size by only by one atom may have quite different structures.

In spite of the large number of calculations performed by a variety of state-of-the-art *ab initio* and density-functional methods, which have somewhat clarified the structural changes of silicon clusters with increasing size, fundamentally interesting and long-standing questions regarding the "non-diamond to diamond structure transition" for bare silicon clusters still remain unanswered. In particular, the critical cluster size at which such a transition occurs has not been conclusively determined. Simulation of small clusters of ten or fewer silicon atoms using pseudopotential-density-functional techniques and extrapolation of the results to large clusters[11] led to an early estimate of over 4000 atoms for the critical size for this transition. In contrast, early tight-binding calculations[12] estimated this size to be only 50 silicon atoms. More recent tight-binding calculations[13] give a somewhat intermediate result for the critical size, 400 atoms.

It is interesting to note that there are scanning probe experiments that seem to support both small[14] and large critical sizes.[15] This suggests that the observed structure of bare clusters may depend on synthesis conditions, and experimentally, one may obtain different cluster structures even in the same size range. This seems to be the case for hydrogen saturated clusters as well, as demonstrated for 1 nm diameter clusters using accurate *ab initio* calculations.[8]

From a theoretical point of view, the exponential growth of the number of possible isomers of clusters with increasing size makes testing and comparing them directly unrealistic, even with tremendous computational resources, especially for *ab initio* methods. Nevertheless, such tasks currently can be performed to some extent by tight-binding calculations. Recently, density-functional-based tight-binding simulations were performed[16] for several hundred isomers of Si_{25}, Si_{29}, and Si_{35} to explore prolate-to-spherical shape changes in this size range. In addition, by considering a few isomers of larger clusters (Si_{71} and Si_{239}), using a simulated annealing approach, and preferring amorphouslike structures with several overcoordinated atoms and cohesive energies significantly lower than that of the bulk, it was concluded that the transition to the ideal diamond structure should occur for cluster sizes much larger than 239 Si atoms.

While simulated annealing is an extremely valuable approach for many practically interesting cases, it may not reliably identify ideal low-energy structures simply because of the impracticality of reaching the slow cooling regimes re-

quired to obtain such structures. On the other hand, in real clusters with a limited number of atoms, amorphous structures with nonregular shapes can be preferred to ideal structures from a free energy point of view, even when the ideal structure has higher cohesive energy. Therefore, nonbulk to bulk structure transitions can be considered an academic question that is best resolved first for zero temperature, and later extended to include finite temperature (entropic) effects. In short-range simulated annealing calculations of large clusters, key fragments of surface layers, like capped pentagons, may appear spontaneously, but irregularly, and will often be masked by disorder. On the other hand, medium-size clusters have been frequently constructed by combining small "magic" compact clusters in the range Si_6-Si_{11} (except Si_8) or polygons, linked by "glue units"[17] made of a diamond structure fragment. This, to some extent, reflects experimental observations,[10] where some of the above magic clusters appear as dissociation products.

Our approach to identifying the transition from nondiamond to diamond structure is to make a thorough comparison of clusters from two distinct families, systematically constructed using the above-mentioned key fragments. This is methodologically more straightforward than searching for a prevalence of diamond fragments over non-diamond ones in the evolution of randomly constructed clusters or tracing the approach of the cohesive energy of such clusters to the bulk value. Recently, we proposed[18] a pentagon-based quasi-one-dimensional growth pattern of silicon clusters that appears to be energetically competitive with the growth pattern established by *ab initio* calculations[10] in the range of cluster sizes up to 20 atoms. Here, the clusters from this growth pattern are taken to represent the lowest-energy non-diamond structures for larger clusters as well, and they are chosen for comparison with clusters having a diamond-like core.

The next section briefly describes computational details and the approach used for constructing clusters. The computational method is the nonconventional tight-binding (NTB) method[18] recently developed and parametrized to *simultaneously* describe the geometry and both cohesive and spectroscopic energies (ionization potentials and electronic affinities) of silicon clusters with accuracy comparable to that of the state-of-the-art *ab initio* methods. No other tight-binding model has been able to do this using a single parametrization scheme. Furthermore, NTB gave good predictions of bulk silicon properties (cohesive energy, lattice constant, band gap, etc.)[18] using a parametrization based entirely on properties of atoms and small clusters. All of these increase our confidence in property predictions for clusters much larger than those used in the parametrization.

Optimization of clusters with a diamond-like core was performed by molecular-dynamics simulations with periodic removal of kinetic energy, which ultimately leads to local energetic minima. This approach was designed to preserve the idealized structures as described above, rather than to search broadly for a global minimum energy structure. Initial structures were constructed using two distinct approaches, dimerization and overcoordination of surface layers, both of which eventually led to pentagon-based surface motifs in the optimized structures. In the case of nondiamond clusters, we also aimed for local minima that followed the ideal pentagon-based regular one-dimensional growth pattern, but distorted clusters eventually appeared to be favorable. Both results are due to a nontrivial competition of surface and core reconstructions in the clusters. The results obtained are discussed in Sec. III. Section IV summarizes the key findings.

II. COMPUTATIONAL DETAILS

The total energy functional of NTB is[18]

$$E_{tot} = \sum_{\mu} \sum_{\nu>\mu} \frac{Z_{\mu}^{scr} Z_{\nu}^{scr}}{R_{\mu\nu}} + \sum_{\mu} \sum_{\nu>\mu} \frac{Q_{\mu} Q_{\nu}}{R_{\mu\nu}} + \sum_{\mu} \sum_{\nu>\mu} \sum_{i} \sum_{j} P_{\mu i,\nu j} H_{\mu i,\nu j} + \sum_{\mu} (E_{\mu} - E_{\mu}^{0}), \quad (1)$$

where $R_{\mu\nu}$ is the internuclear distance,

$$Z_{\mu}^{scr} = Z_{\mu}^{scr}(R_{\mu\nu}, \{N_{\mu i}^{0}\}) = Z_{\mu} - \sum_{i} N_{\mu i}^{0} \left[1 - a_{\mu i} \exp\left(- \frac{\alpha_{\mu i} R_{\mu\nu}}{R_{\mu i}^{0}} \right) \right], \quad (2)$$

$$Q_{\mu} = Z_{\mu}^{scr}(R_{\mu\nu}, \{N_{\mu i}^{0}\}) - Z_{\mu}^{scr}(R_{\mu\nu}, \{N_{\mu i}\}) \quad (3)$$

are screened nuclear and nonpoint ionic charges, respectively, Z_{μ} is the charge of the μth nucleus (or nucleus plus core electrons), $R_{\mu i}^{0} = n_{\mu i} / \xi_{\mu i}^{0}$ is the most probable distance between the ith electron and the corresponding μth nucleus, $n_{\mu i}$ and $\xi_{\mu i}^{0}$ are the principal quantum number and Slater exponent of the ith atomic orbital (AO) centered at the μth nucleus, E_{μ}^{0} and E_{μ} are the total energies of individual atoms in noninteracting and interacting systems characterized by sets of occupancy numbers $\{N_{\mu i}^{0} \equiv P_{\mu i,\mu i}^{0}\}$ and $\{N_{\mu i} \equiv P_{\mu i,\mu i}\}$ and energies $\{E_{\mu i}^{0}\}$ and $\{E_{\mu i}\}$ of valence AOs, respectively, and α and a are fitting parameters.

AOs are presumed to be orthogonal, and a secular equation $\Sigma_{\nu j}(H_{\mu i,\nu j} - \varepsilon \delta_{\mu i,\nu j}) C_{\nu j} = 0$ is solved self-consistently to obtain electronic spectra $\{\varepsilon_k\}$ and AO expansion coefficients $\{C_{\nu j}(k)\}$ of the molecular orbitals of the system. Self-consistent calculations are performed by iterative recalculation of diagonal elements of the Hamiltonian matrix elements $H_{\mu i,\mu j}$ using the dependence of the bond-order matrix and AO occupancy numbers $N_{\mu i} \equiv P_{\mu i,\mu i}$ on $C_{\nu j}(k)$.

For other formulas and details of NTB, see Ref. 18. Here, we should note the following. NTB uses a total energy functional that is different in form from commonly used tight-binding (TB) energy functionals. NTB uses a different definition of the repulsive energy term [the first term in Eq. (1) in the non-self-consistent calculation case] with simple physical content; it is the sum of the repulsion energy between nuclei and half of the attraction energy of electrons to "foreign" nuclei, and thus, can be represented more reliably by short-range pairwise functions of interatomic distances than the repulsive term in other TB models. Moreover, accurate and detailed parametrization of ionization and promotion energies of atoms and ions is a principal difference between NTB and traditional TB models, enabling one to account adequately for the majority of correlation effects in multiatomic systems as well. Using these features, we have been

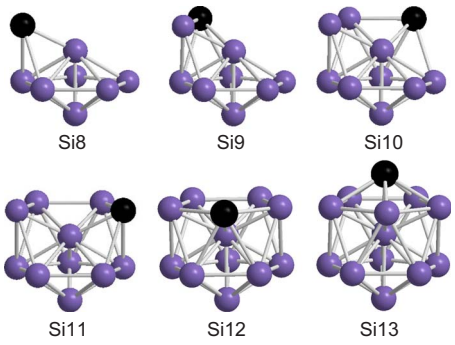

FIG. 1. (Color online) The pentagon-based one-dimensional growth pattern (Ref. 18) illustrated for clusters Si_8–Si_{13}. The newly added atom (see text) is shown as a black ball in each case. Construction of larger clusters through repetition of this pattern is straightforward.

able to extend NTB far beyond the capabilities of traditional TB for describing geometries, cohesive energies, ionization potentials, and electronic affinities of bare silicon[18] cluster containing up to 20 atoms, as well as atomization energies of more than 130 silicon-hydrogen[19] clusters with accuracy comparable to state-of-the-art *ab initio* methods. The computational approach used here is a combination[18] of this NTB with molecular-dynamics simulations based on an accurate algorithm[20] for the integration of the equations of motion.

In describing cluster structures, we use coordination numbers (CNs) of atoms defined by a simple distance criterion. Namely, every atom within a distance R_c around a given atom will be considered as one of its first-nearest neighbors. Thus, for example, a three-coordinated atom has three other atoms within a distance R_c and its coordination number is 3; sometimes we use the term "number of bonds" with the same meaning. To diminish the effect of such a sharp stepwise criterion, we choose a relatively large value of R_c=2.80 Å in most cases. In some cases, we use the value R_c=2.65 Å, which was more effective for distinguishing non-diamond and diamond-like clusters (see next section).

Si_7 with a bicapped pentagon geometry is the starting cluster for the non-diamond one-dimensional growth pattern.[18] In this cluster, all interatomic distances are below 2.51 Å,[18] except for the distance between nonadjacent atoms in the pentagon. Thus, for atoms in the pentagon CN=4, and for apex atoms CN=6. This cluster can grow by sequential addition of silicon atoms as follows. The first atom can be placed above or below the pentagon of Si_7, where it will have three neighbors (two from the pentagon and one of the two capping atoms) at distances smaller than R_c, so CN=3 (Fig. 1, Si_8). Upon addition of another Si atom adjacent to that one (Fig. 1, Si_9), both added atoms become four-coordinated. Each of the next two atoms added is four-coordinated and increases the coordination number of the previous atom by 1. The fifth added atom forms an additional bond also with the first atom added, completing another pentagon (Fig. 1, Si_{12}). Capping this pentagon with a sixth atom gives an icosahedral cluster (Fig. 1, Si_{13}), increasing the number of bonds (or CN) by 1 for each atom in the new pentagon. As a result, the CN of all atoms becomes 6, except the atom at the center of the icosahedron which now has CN=12. This is an unusually high CN for Si, and the central atom in the icosahedral cluster can be considered to be in a strained position. The cluster Si_{13} with this central atom removed, that is, Si_{12}, appears to be about 0.1 eV/atom lower in energy than Si_{12} with geometry shown in Fig. 1. The cohesive energy per atom for three clusters Si_{12}, Si_{13}, and Si_{14} in Fig. 7 of Ref. 18 appeared practically to be the same, ~3.95 eV.

In order to reduce calculations, here we consider primarily clusters of Si_{13+6n} type with completed and capped pentagons, which can be obtained by sequentially adding the capped pentagonal motif to Si_{13}, Si_{19}, etc., and which have only one representative for each cluster size if one disregards distortions. These clusters, from the point of view of maximizing CN, are expected to be favorable. However, they are not necessarily energetic mimina because of the increasing number of strained atoms in their interior. The above-mentioned example of a hollow icosohedral Si_{12} cluster suggests that one might achieve increased stability of clusters from this pattern by removing internal atoms from Si_{19}. Consideration of a few larger clusters, however, did not support this expectation. It seems that having more weak bonds for surface atoms with CN=6 is more important for larger clusters of this pattern. Removing internal atoms reduces the number of bonds of all surface atoms, except those in two edge pentagons, to 4. While this is equal to that in a bulk diamond-like structure, it is much less favorable because of the strong deviation from the ideal tetrahedral coordination. Nevertheless, more or less distorted clusters of the pattern appeared to be favorable relative to idealized structures of the pattern. The latter often caused convergence problems in self-consistent calculations, which disappeared upon introduction of a small distortion to the original higher symmetry structures. Relaxation of such structures to the lowest possible local minimum required substantial simulation times for large clusters. Therefore, the structures shown in the next section (Figs. 3 and 4) were actually optimized starting from initial structures that were obtained by adding a pentagonal motif (again not necessarily with perfect symmetry) to a distorted structure of a previous cluster. Note that the first cluster in our series, Si_{19}, obtained analogously in Ref. 18, which we started from was already distorted. Molecular-dynamics optimization of such clusters took simulation times of up to 5000 fs at a time step of 1 fs.

The clusters, constructed as described above, were optimized to local energetic minima as follows. A constant energy molecular-dynamics simulation was started from the initial geometry. The kinetic energy of the system increases as the potential energy decreases. After the geometry passes through (or near) an energetic minimum, the potential will begin to increase and, therefore, the kinetic energy will decrease. When such a decrease in kinetic energy was observed, the velocities of the atoms were set to zero (all kinetic energy was artificially removed). The constant energy molecular-dynamics simulation then resumed at a new, lower, total energy. This heuristic approach is effective for guiding the simulation toward a local minimum near the starting geometry without trapping the structure in the absolute closest local minimum (as, for example, might happen

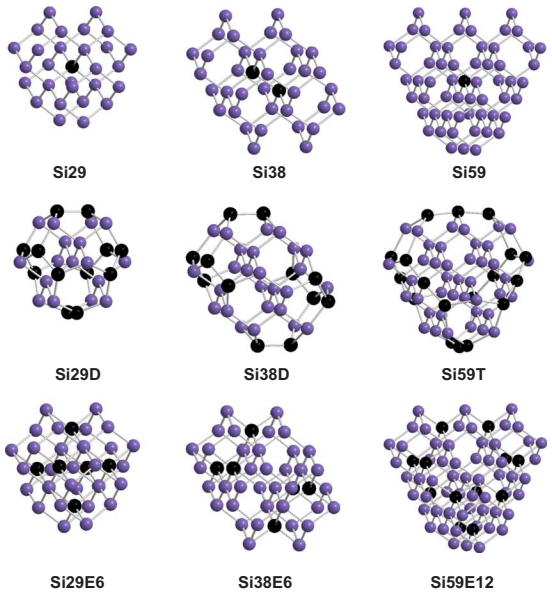

FIG. 2. (Color online) Three prototypical diamond-like clusters: Si_{29} centered on a single atom (Si29), Si_{38} centered on a Si–Si bond (Si38), and Si_{59} centered on a single atom (Si59), respectively, which were used as the basis for clusters with a diamond-like core. Also shown are the corresponding idealized structures with dimerization (Si29D and Si38D) or trimerization (Si59T) of the two-coordinated surface atoms, and clusters with additional atoms embedded beneath the surface to increase the coordination number of surface atoms (Si29E6, Si38E6, and Si59E12). The atoms of interest in each case [central atom(s) in the top row, dimerized or trimerized atoms in the second row, and embedded atoms in the third row] are shown as black balls.

with a pure steepest-descent optimization). In order to refine the minimum energy geometry, the kinetic energy was typically removed at least ten times, with the geometry approaching the exact minimum more closely after each energy dissipation. Calculations were repeated for many different starting configurations. Comparing the total energy of clusters thus obtained allows one to identify both local and likely global minimum energy configurations. The energy dissipation was not usually done for the first few passages through minima at the beginning of a simulation to avoid trapping the structure in the first, possibly shallow, minimum encountered. Typically, the first few dissipations of kinetic energy removed at least 0.5–1 eV from the cluster. The simulation was terminated when the maximum kinetic energy of the cluster was less than 0.001 eV. Starting geometries had about 3–7 eV higher energies than final geometries, so that each cluster originally had enough potential to avoid most shallow minima, even without heating them to high temperatures as in simulated annealing approaches.

Molecular-dynamics optimization of diamond-like clusters was performed analogously, but without lowering their symmetry. In this case, we started from three prototype clusters (Fig. 2) cut from the bulk silicon structure, consisting of 29, 38, and 59 atoms, respectively. The large number of surface atoms with CN$<$4 makes these clusters energetically unfavorable compared to compact or overcoordinated (CN $>$4) structures. The most undesirable surface atoms in the clusters shown in Fig. 2 are two-coordinated atoms. To eliminate them, we simply form dimers or trimers from them; the former are well-known, usually buckled, structures on the (100) surface of bulk silicon and seem to be necessary even in the case of small hydrogen-saturated clusters.[8] We also created another set of clusters, embedding additional atoms into the surface of the prototype clusters in such a way that each of them occupied a position that would correspond to a tetrahedral interstitial position in bulk silicon (Fig. 2). This increases the CN of surface atoms and is, therefore, expected to increase the cohesive energy of clusters with large surface to volume ratio. We also constructed a few more clusters based on the optimized geometries of the initial structures by removing some surface atoms with CN=3 (4) in possibly strained configurations.

III. RESULTS AND DISCUSSION

A. Pentagon-based one-dimensional clusters

Figures 3 and 4 depict the geometries of optimized clusters from the regular growth pattern, containing up to 61 atoms. Several characteristics of these clusters are given in Table I. As shown in Figs. 3 and 4, the larger clusters are

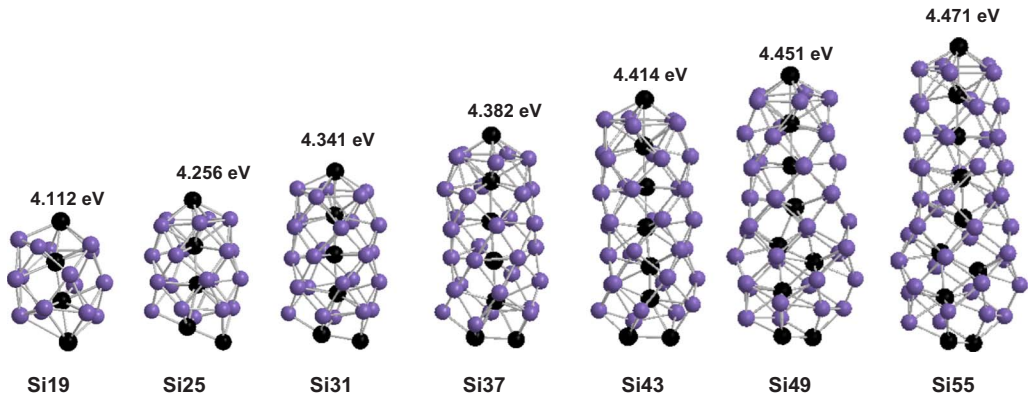

FIG. 3. (Color online) Optimized geometries of quasi-one-dimensional non-diamond clusters (see also Fig. 4). The cohesive energy per atom for each cluster is also given. Atoms that would lie on the axis of the idealized stacked pentagon structure are shown as black balls.

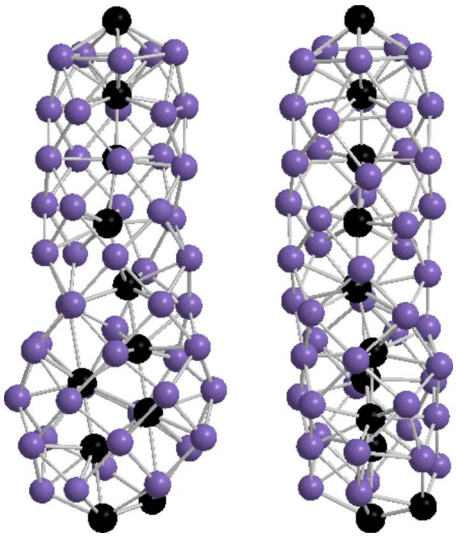

FIG. 4. (Color online) Two views of the optimized geometry of the Si_{61} cluster (cohesive energy per atom is 4.50 eV) showing the quasi-two-dimensional character of one end of the cluster.

significantly distorted and do not perfectly follow the growth pattern illustrated in Fig. 1. The distortion increases with increasing cluster size due to accumulation of strain in the bonds between the silicon atoms along the central axis of the clusters. These atoms are shown as black balls for clarity. In the idealized clusters, these bonds are much shorter than expected for their given coordination numbers (12) and were closer to the bond length in Si_2 (~2.25 Å). Such short distances were forced by the binding of surface atoms from different pentagons. The distances between these atoms, unlike the distances between atoms on the central axis, were as expected (≥2.35 Å) given their coordination numbers (5 or 6).

Thus, the competition between increasing the cluster cohesive energy by establishing optimal bond lengths and angles for the surface atoms vs decreasing this energy due to constraint of the atoms along the cluster central axis to suboptimal bond lengths governs the behavior of this nondiamond one-dimensional growth channel. The shrinking of the clusters' surface along the growth direction forces the atoms on the central axis closer to each other. To diminish their repulsive interactions, these atoms deviate from their ideal locations in a straight line on the cluster axis. As a result, they tend to form a zigzag, which, in turn, leads to distortion and expansion of the pentagons formed by surface atoms. However, there is limited space for the formation of this zigzag pattern within the interior of small clusters. This causes very strong distortion of one end of the Si_{25} cluster, preventing this end from growing further via the capped pentagon motif. In the larger clusters, this end then serves as sink for accommodating further bond strain. In the Si_{49} cluster, it incorporates a two-dimensional four-atom motif within its interior. In the Si_{61} cluster, this end has become almost fully two-dimensional (Fig. 4). This cluster has the largest binding energy per atom (4.5 eV, which is ~0.13 eV lower than the value for bulk silicon) among clusters considered.

As noted before, the removal of internally strained atoms does not lead to greater stability of Si clusters, because these atoms are necessary for stabilizing surface atoms. This contrasts with the case of carbon nanotubes, for which such stabilization is known to be due to strong π-π bonds of carbon. At the same time, these strained atoms initiate the above described competition between surface and core reconstructions. As a result, the average CN of all optimized clusters was decreased relative to the ideal cluster, due to significant increase of most interatomic distances. Generally, no more than one atom in the optimized clusters had CN =12, which is characteristic of the atoms along the axis of the ideal cluster. Moreover, one or two atoms in clusters with the number of atoms between 13 and 49 had CN=3 (clearly seen for Si_{25} in Fig. 3).

The further addition of atoms to the above clusters, of course, not necessarily according to the pattern shown in Fig. 1, is of particular interest, because in this way one may be able to observe a transformation of the above clusters to three-dimensional ones with a diamond-like core. However, simulations performed for the Si_{67} cluster constructed according to the pattern in Fig. 1 and for several other clusters with Si atoms added to the Si_{61} cluster at peripheral positions did not significantly increase the binding energy relative to Si_{61}. Thus, this size seems to be a critical one, above which more dramatic changes must occur in the core of the nondiamond clusters. This remains to be explored in more detail.

TABLE I. Average CN, nearest-neighbor distance (R_{aver}), length (l), and HOMO-LUMO gap (ΔE) of pentagon-based quasi-one-dimensional clusters.

Cluster	Si19	Si25	Si31	Si37	Si43	Si49	Si55	Si61
CN_{aver}	5.368[a]	5.760	5.677	5.676	5.674	5.918	5.673	5.738
	5.368[b]	5.280	5.419	5.514	5.488	5.714	5.600	5.508
R_{aver} (Å)	2.444[a]	2.454	2.442	2.443	2.440	2.447	2.433	2.435
	2.444[b]	2.423	2.432	2.435	2.432	2.438	2.429	2.425
l[c] (Å)	6.704	8.562	9.995	11.574	13.280	14.472	16.221	17.251
ΔE (eV)	0.343	0.286	0.254	0.407	0.187	0.118	0.200	0.167

[a]The first row for R_c=2.80 Å.
[b]The second row for R_c=2.65 Å.
[c]The largest interatomic distance.

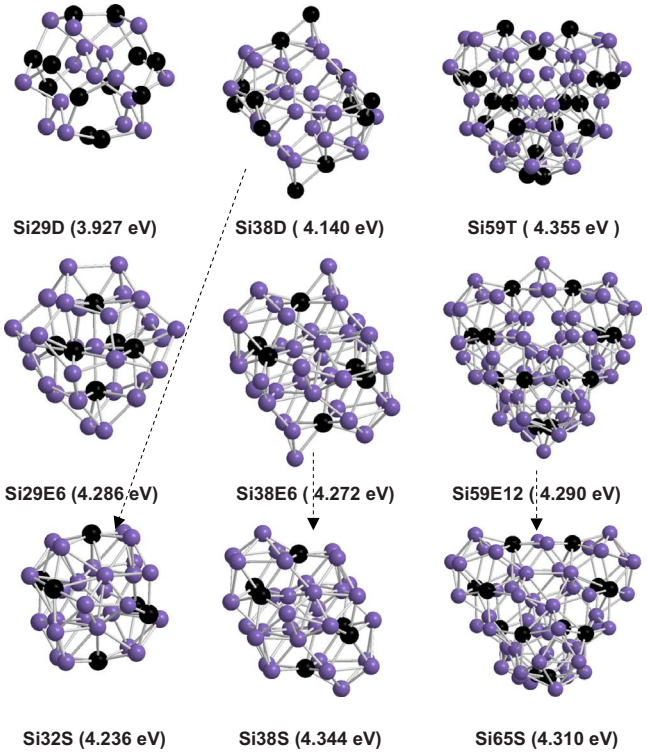

FIG. 5. (Color online) Optimized geometries of clusters Si29D, Si38D, Si59T, Si29E6, Si38E6, and Si59E12 from Fig. 2. Clusters Si32S, Si38S, and Si65S are optimized geometries of clusters that were derived from Si38D, Si38E6, and Si59E12, respectively, by removing six vertex atoms in each case to smooth the cluster surface. The cohesive energy per atom is given in parentheses for each structure.

B. Clusters with an initially diamond-like core

The optimized geometries of clusters that initially had a diamond-like core are depicted in Fig. 5. Three additionally derived geometries are also shown, based on the removal of vertex atoms from optimized clusters. Several characteristics of these clusters are given in Table II. One can see a significant shrinking of the surface formed by dimerized atoms in the cluster Si29D; the distance between them and the central atom is 3.43 Å in the optimized geometry, which is significantly shorter than the second-nearest-neighbor distance in bulk silicon, 3.83 Å. Bond distances between the dimerized atoms and neighboring surface atoms are only 2.266 Å. Other bonds are ~2.31 Å in length and form a nearly ideal diamond-like structure. In the overcoordinated cluster Si29E6, the central atom completely lost its tetrahedral coordination. In the optimized structure, it has octahedral coordination due to the inversion of the positions of the six embedded atoms and the four initial nearest-neighbor atoms of the central atom. The distance between the central atom and its six octahedrally coordinated neighbors is only 2.245 Å, while the length of other bonds is above 2.35 Å.

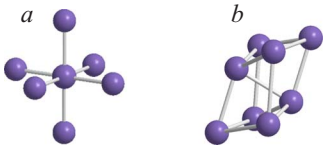

FIG. 6. (Color online) The resulting core geometries of (a) Si29E6 and Si38E6, and (b) Si38S and Si32S.

The dimerized cluster Si38D showed strong surface (Fig. 5) and core reconstructions (Fig. 6) that led to the formation of capped pentagon motifs on the surface. The latter was possible because of strong buckling of dimers, such that one of the atoms in each pair became a three-coordinated vertex atom. The distance between the two central atoms is 2.293 Å. We derived cluster Si32S from Si38D by removing the six three-coordinated vertex atoms and optimizing the geometry of the resulting cluster. This increased the cohesive energy per atom, in spite of the decrease in the number of atoms. All bond distances became larger than 2.32 Å, and the distance between the two central atoms was 2.46 Å.

In the cluster Si38E6, one can see again both strong surface (Fig. 5) and core (Fig. 6) reconstructions, and capped pentagon motifs and three-coordinated vertex atoms. In this cluster, the pairs of outermost atoms that initially had two dangling bonds apiece were displaced so that one member of each pair became a three-coordinated vertex atom, while the other became the capping atom of a capped pentagon. The two central atoms lost their tetrahedral coordination. The distance between them is 2.41 Å, while the distance between

TABLE II. Average CN, nearest-neighbor distance (R_{aver}), diameter (D), and HOMO-LUMO gap (ΔE) for clusters initially having a diamond-like core.

Cluster	Si29D	Si38D	Si59T	Si29E6	Si38E6	Si59E12	Si32S	Si38S	Si65S
CN_{aver}	3.172[a]	5.105	5.017	5.486	5.500	5.521	5.687	5.737	5.662
	3.172[b]	4.474	5.017	5.143	4.682	4.845	4.562	4.789	4.554
R_{aver} (Å)	2.285[a]	2.417	2.434	2.444	2.458	2.452	2.480	2.469	2.463
	2.285[b]	2.381	2.434	2.429	2.421	2.412	2.426	2.420	2.405
D[c] (Å)	7.826	10.426	10.592	8.553	10.435	11.622	7.879	9.814	11.228
ΔE (eV)	0.028	0.098	0.166	0.523	0.149	0.03	0.217	0.463	0.083

[a]The first row for R_c=2.80 Å.
[b]The second row for R_c=2.65 Å.
[c]The largest interatomic distance.

them and their other first neighbors is 2.48 Å. The shortest bond distance between peripheral atoms is 2.323 Å. In the cluster Si38S, smoothened by removing the six vertex atoms from Si38E6, the cohesive energy per atom again increases. The main geometrical change is that the distance between two central atoms became 2.322 Å, which almost coincides with the shortest bond distance in the cluster, 2.315 Å.

In the trimerized cluster Si59T, the distance between the central atom and its first neighbors is 2.309 Å. Other bond distances are larger than 2.32 Å. Here, on the surface region (Fig. 5), one can recognize a somewhat modified fragment of clusters from the pentagon-based one-dimensional pattern (Figs. 3 and 4). Cluster Si59E12 and its derivative, Si65S, also have such a fragment, but larger in size and with a different orientation. Note, however, that in all three clusters (Si59T, Si59E12, and Si65S) these fragments do not involve internal axial atoms like those in the clusters shown in Figs. 3 and 4. In the optimized geometry, the central atom in each trimer (Si59T, see Fig. 2) became embedded into the cluster (Fig. 5) after geometry optimization. As a result, the final structure represents a combined realization of the two types of cluster construction described in the previous section. Surface smoothing has a strong influence on internal bond distances in the case of Si59E12 as well. The distance between the central atom and its first neighbors in the smoothened cluster Si65S (2.373 Å) became noticeably larger than that in Si59E12 (2.279 Å).

Dimerized clusters have smaller cohesive energies per atom than other clusters. However, the trimerized cluster, Si59T, which exhibits a combination of the two growth motifs has the largest cohesive energy per atom, 4.355 eV. This was the largest among all initially diamond-like clusters considered, including those with a larger number of atoms. The first set of clusters, with dimerized or trimerized surface atoms (Si29D, Si38D, and Si59T), can be considered as representatives of clusters with a diamond-like core: they each have tetrahedrally coordinated atoms at their core. The first two clusters in each of the other sets, (Si29E6, Si38E6) and (Si32S, Si38S), cannot be considered diamond-like because they do not retain tetrahedrally coordinated atoms at their core (Fig. 6). Moreover, energies of clusters from these two sets do not show any regular dependence on the number of atoms in the cluster (Fig. 7). They have an average CN larger than the first set of clusters (Table II). The trend in CN for the three sets is substantially changed when R_c=2.65 Å is used (rather than R_c=2.8 Å), which indicates that sets of clusters that did not retain a diamond-like core have, on average, more elongated bonds (larger than 2.65 Å) than the first set of clusters.

C. Comparison of non-diamond and diamond-like clusters

The largest cohesive energy per atom (4.355 eV) for representative diamond-like clusters was observed for Si59T. This value is smaller than that for non-diamond clusters (4.50 eV), which demonstrates that non-diamond cluster structures remain energetically preferable over the entire size range considered here. In addition, we observed (Fig. 5) key surface fragments in energetically competitive larger

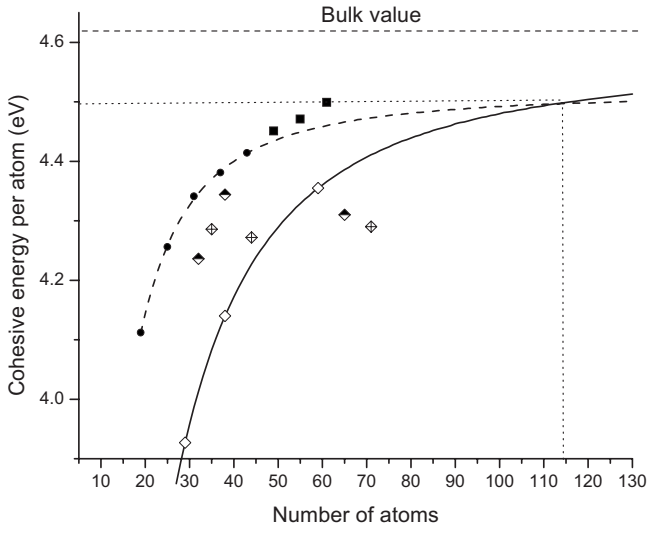

FIG. 7. Cohesive energy per atom for non-diamond one-dimensional clusters (black dots and filled rectangles) and clusters with originally diamond-like core (diamonds). Open diamonds correspond to representative diamond-like clusters (Fig. 5, first row), crossed diamonds to clusters with originally surface embedded atoms (Fig. 5, second row), and half-filled diamonds to surface smoothened clusters (Fig. 5, third row). Filled rectangles correspond to non-diamond clusters with a quasi-two-dimensional end.

diamond-like clusters that include capped pentagons. These surface structures appear to be more favorable than simple dimers (trimers) or capped trimers or tetramers. The cluster Si59T (Fig. 5), with a surface dominated by capped pentagons, has a larger cohesive energy per atom than the larger clusters Si59E12 and Si65S. The clusters Si38D, Si38E6, and Si59E12 have both capped pentagons and capped trimers (or tetramers), but removing the latter, while retaining capped pentagons, increases their cohesive energy per atom in spite of decreasing the number of atoms. Thus, capped pentagons are key fragments. They are energetically favorable not only because they introduce more bonds, but also because of diminished strain resulting from increased bond angles compared to capped trimers and tetramers. Therefore, the surface regions of large diamond-like clusters are expected to be reconstructed such that they consist of pentagon-based fragments attached to a core fragment of diamond-like structure. From this point of view, it is rational to start from clusters constructed as linked pentagon-based fragments and ideal diamond structures, and not from dimerized or trimerized structures like those in Fig. 2. Such an approach may also help to avoid the problem of being trapped by intermediate surface structures. Alternatively, from the start of computer simulation, it is necessary to provide atoms on the surface with quite high velocities (kinetic energies to overcome possible barriers) in proper directions (not random as in simulating annealing). Figure 8 demonstrates how the armchair fragment of a diamond structure can transform into a capped pentagon. It is also worth noting that edge reconstruction models of silicon nanowires (see, for instance, Ref. 21) can also obviously benefit from capped pentagon motif.

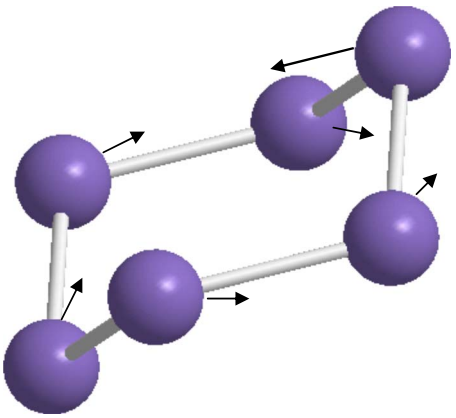

FIG. 8. (Color online) Schematic displacement modes for atoms in the armchair fragment of diamond structure for transforming this fragment into a capped pentagon.

Although calculations on larger clusters are clearly needed to definitively identify a transition from non-diamond to diamond-like clusters, we can estimate this transition point based on results presented here. This requires extrapolating the cohesive energy per atom of representative clusters for larger cluster sizes. Because this energy must asymptotically approach the bulk cohesive energy for diamond-like clusters, this procedure is quite safe, provided that an analytical function with proper behavior is chosen. Such a function behaves like a Fermi distribution function, so we tried several such functions, including

$$E_{coh} = E_\infty - E_\infty / \{1 + [(N-1)/\tilde{N}]^q\}, \tag{4}$$

where N is the number of atoms in the cluster and E_∞ is a saturation value of cohesive energy per atom when $N \to \infty$. E_∞, $\tilde{N}$, and q are fitting parameters. This function is meaningful for $N \geqslant 1$ and is equal to zero for the single isolated atom. If, by fitting cohesive energies of clusters alone, one obtains E_∞ coinciding with the bulk value, this suggests that an appropriate function has been chosen, and the clusters used in the fitting are reasonable representatives of diamond-like clusters. If fitting to the cluster energies does not result in a reasonable value for the bulk cohesive energy, then either the function is not appropriate or the selected clusters are not representative. With respect to the clusters, this means that they may still be too small to incorporate enough tetrahedrally coordinated atoms and their energy may be dominated by the relatively large number of surface overcoordinated atoms.

Clusters Si29D, Si38D, and Si59T, as discussed above, are taken as representatives of diamond-like clusters. Two other larger clusters Si65S and Si59E12 with a diamond-like core have lower cohesive energies than Si59T, therefore we do not include their energies for fitting. For these reasons, and because the distorted non-diamond clusters shown in Figs. 3 and 4 can be realized in many ways with similar energies, and therefore, are favored from an entropic point of view, our estimation is expected to be a lower bound for the transition. In the case of Eq. (4), we obtained the following values of the fitting parameters:

$$E_\infty = 4.573 \text{ eV}, \quad \tilde{N} = 9.852, \quad q = 1.672.$$

The three-parameter fitting with these values exactly reproduces the cohesive energies of the three representative clusters and, in addition, E_∞=4.573 eV almost coincides with the bulk cohesive energy obtained by NTB,[18] 4.582 eV. Other candidate functions did not achieve such accuracy in the extrapolation to infinite N, giving significantly deviating saturation values (in particular, ~4.38 eV in the case of an exponential function). Thus, a lower bound of critical cluster size for non-diamond to diamond transition can be estimated to be about 115 atoms (Fig. 7), and the binding energy per atom of clusters at this transition point is about 4.50 eV, which surprisingly coincides with the largest energy of non-diamond clusters, achieved for Si_{61}. It is interesting also to note that the subset of non-diamond clusters without a two-dimensional end, when approximated by Eq. (4), is described by the curve that crosses at the same point.

The estimation of the highest occupied molecular orbital (HOMO) lowest unoccupied molecular orbital (LUMO) gap for small nonsaturated silicon clusters by scanning tunneling spectroscopy measurements[15] found two distinct size regions: between 2.5 and 15 Å, clusters show energy gaps up to 0.45 eV, while above 15 Å, only zero (or almost zero) gaps were observed. At the same time, in the first size region, the energy gap does not monotonically increase with decreasing size, and there are clusters with zero gaps in this region as well. The HOMO-LUMO gaps of the clusters calculated here (Tables I and II), belonging mainly to the small-size regime, are in qualitative agreement with this experiment, reflecting the nonregularity of the gap with cluster size and a similar maximum gap of 0.407 eV (Table I) or 0.523 eV (Table II).

The above observation of irregularities in the band gap is not surprising, given the existence of undercoordinated atoms (or dangling bonds), defects, and strained atoms in both cluster types, which usually introduce surface localized levels into the HOMO-LUMO gap. Dimers are also known[22] to introduce such levels and, therefore, dimerization-based surface reconstruction models in nanowires,[21] belonging to the large-size regime, can explain the metallic or semimetallic behavior of the latter.

Finally, from Tables I and II, one can see the sensitivity of CN to the choice of R_c. Using R_c=2.65 Å, the difference between non-diamond clusters and clusters with originally diamond-like core is clearly seen: the latter have average CN below 5 or just around 5, while non-diamond clusters have average CN mostly closer to 6. At R_c=2.65 Å, average nearest-neighbor distances (bond lengths) are practically the same in both cluster types and about 0.06 Å higher than the bulk value. This can be explained by the existence of a relatively large number of overcoordinated atoms in both types of clusters.

IV. CONCLUSION

In summary, silicon clusters with a diamond-like core and non-diamond cluster structures were simulated and com-

pared using the nonconventional tight-binding molecular-dynamics simulation method.[18] Non-diamond clusters were constructed according to a pentagon-based regular growth pattern proposed previously.[18] For clusters with a diamond-like core, energetically unfavorable dangling bonds were partially eliminated by dimerization (trimerization) of Si atoms with two dangling bonds and/or overcoordination of surface atoms. A nontrivial competition of surface and core reconstructions in the clusters, in order to reach energetically favorable atomic arrangements, was observed, accompanied by distortions and partial amorphization of the initially highly regular and symmetric structures. This eventually restricts the one-dimensional growth of clusters of the regular growth pattern from both geometrical and energetic points of view. The maximum cluster size for this pattern is about 61 atoms. However, starting from the cluster Si_{49}, one end of these clusters became rather two-dimensional. In the range of cluster sizes ($\leq$71 atoms) considered, clusters with a diamond-like core are energetically unfavorable compared to representative non-diamond clusters from the pentagon-based quasi-one-dimensional growth pattern. Optimized geometries of the structures with a diamond-like core were sensitive to the initial surface reconstruction model. In several cases, these cluster geometries converged to structures that no longer contained a diamond-like core. The importance of capped pentagon motifs in surface reconstruction for energetically competitive nanometer-size diamond-like clusters was demonstrated. The results obtained here can be extrapolated to estimate a lower bound for the transition from the non-diamond structure to diamond-like structure of about 115 atoms for pure silicon clusters.

ACKNOWLEDGMENTS

The research described in this paper was made possible in part by the Uzbek Academy of Sciences Fund for Supporting Fundamental Research (No. 6-06) and the U.S. National Science Foundation (Grant No. CTS-0500249). P.L.T. was supported by CRDF 10ANNJSF (Grant No. UZC1-2671-TA-05).

*Corresponding author; pltereshchuk@mail.ru
†Deceased.

[1] L. T. Canham, Appl. Phys. Lett. **57**, 1046 (1990).
[2] G. Belomoin, J. Therrien, A. Smith, S. Rao, R. Twesten, S. Chaieb, M. H. Nayfeh, L. Wagner, and L. Mitas, Appl. Phys. Lett. **80**, 841 (2002).
[3] M. V. Wolkin, J. Jorne, P. M. Fauchet, G. Allan, and C. Delerue, Phys. Rev. Lett. **82**, 197 (1999).
[4] J. P. Wilcoxon, G. A. Samara, and P. N. Provencio, Phys. Rev. B **60**, 2704 (1999).
[5] J. A. Carlisle, M. Dongol, I. N. Germanenko, Y. B. Pithawalla, and M. S. El-Shall, Chem. Phys. Lett. **326**, 335 (2000).
[6] D. S. English, L. E. Pell, Z. H. Yu, P. F. Barbara, and B. A. Korgel, Nano Lett. **2**, 681 (2002).
[7] F. Hua, M. T. Swihart, and E. Ruckenstein, Langmuir **21**, 6054 (2005).
[8] E. Draeger, J. C. Grossman, A. J. Williamson, and G. Galli, J. Chem. Phys. **120**, 10807 (2004).
[9] K. Raghavachari and C. M. Rohlfing, J. Chem. Phys. **89**, 2219 (1988); **96**, 2114 (1992).
[10] K. M. Ho, A. A. Shvartsburg, B. Pan, Z. Y. Lu, C. Z. Wang, J. G. Wacker, J. L. Fye, and M. F. Jarrold, Nature (London) **392**, 582 (1998).
[11] D. Tomanek and M. A. Schluter, Phys. Rev. B **36**, 1208 (1987).
[12] J. R. Chelikowsky, Phys. Rev. Lett. **60**, 2669 (1988).
[13] D. K. Yu, R. Q. Zhang, and S. T. Lee, Phys. Rev. B **65**, 245417 (2002).
[14] P. Mélinon, P. Kéghélian, B. Prével, V. Dupuis, A. Perez, B. Champagnon, Y. Guyot, M. Pellarin, J. Lermé, M. Broyer, J. L. Rousset, and P. Delichére, J. Chem. Phys. **108**, 4607 (1998).
[15] B. Marsen, M. Lonfat, P. Scheier, and K. Sattler, Phys. Rev. B **62**, 6892 (2000).
[16] A. Sieck, Th. Frauenheim, and K. A. Jackson, Phys. Status Solidi B **240**, 537 (2003).
[17] Soohaeng Yoo and X. C. Zeng, J. Chem. Phys. **124**, 054304 (2006).
[18] Z. M. Khakimov, P. L. Tereshchuk, N. T. Sulaymanov, F. T. Umarova, and M. T. Swihart, Phys. Rev. B **72**, 115335 (2005); Z. M. Khakimov, J. Phys.: Conf. Ser. **29**, 177 (2006).
[19] Z. M. Khakimov, P. L. Tereshchuk, N. T. Sulaymanov, F. T. Umarova, A. P. Mukhtarov, and M. T. Swihart, ECS Trans. **2**, 279 (2006).
[20] Z. M. Khakimov, Comput. Phys. Commun. **147**, 731 (2002).
[21] R. Rurali and N. Lorente, Nanotechnology **16**, S250 (2005).
[22] G. Allan, C. Delerue, and M. Lannoo, Phys. Rev. Lett. **76**, 2961 (1996).